TOWARDS GHZ ULTRASOUND ENABLED NONINVASIVE HYDROGEL METROLOGY FOR MECHANOBIOLOGY

Yilmaz Arin Manav[1], Frederick Sebastian[1], Anuj Baskota[2], Justin C. Kuo[2], Rouzbeh Amini[1], Amit Lal[2,3], and Benyamin Davaji[1]*
[1]Northeastern University, USA, and
[2]Geegah LLC, USA, and [3]Cornell University, USA

2024 IEEE 37th International Conference on Micro Electro Mechanical Systems (MEMS) | 979-8-3503-5792-9/24/$31.00 ©2024 IEEE | DOI: 10.1109/MEMS58180.2024.10439458

ABSTRACT

This paper presents a noninvasive method for the measurement of transient mechanical properties for hydrogel swelling using a CMOS-integrated piezo MEMS ultrasound imager operating at ~1.8 GHz. The noninvasive measurement and tuning of hydrogel stiffness is crucial for creating cell culture environments with different mechanical properties to study the mechanical interactions between cells and the surrounding matrix [1]. We present a novel method for real-time and noninvasive measurement of hydrogel swelling using GHz ultrasound reflectometry. We measured five samples from seven different batches with water contents varying from zero (dry) to 1000 µL water per 100 mg of hydrogel—the ultrasound-based measured bulk modulus of hydrogel samples (~1-4.5 GPa) verified by micro indentation showing closely matching trends.

KEYWORDS

GHz ultrasound, ultrasound metrology, Aluminum Nitride ultrasound array, hydrogel elasticity.

INTRODUCTION

Ultrasound has been widely used for imaging biological samples and for quantifying mechanical properties of tissues and organs [2]. However, the chip scale ultrasound arrays (0.5-20 MHz) rarely operate at GHz frequencies due to fabrication challenges such as the compatibility of the piezoelectric materials for the required feature sizes, the power constraints, and the on-chip signal processing required for the number of transducers that can be operated on-chip [3]. As a result, most GHz ultrasound systems are limited to single-pixel transducers or smaller arrays with lower pixel density. Higher frequency (small wavelength) GHz ultrasound inherently has a higher spatial resolution (z-direction), and when combined with the high pixel density of the CMOS integrated piezoMEMS system, provides unmatched spatial resolution measurement in-depth and at lateral dimensions (x and y-directions). GHz ultrasound imager enables the characterization of the mechanical properties of samples in a desirable wide range of micron to mm scale [4].

A single frame of ultrasound data consists of up to ~16k datapoints (full frame), with frames being acquired at a rate of 10-20 frames per second [5]. The number of data points acquired from one frame allows for obtaining a statistically reliable dataset without repeated measurements and sample preparation. Obtaining a large dataset in a single measurement allows straightforward accounting for measurement imperfections that might occur from misreading around the edges or regions where the interface is not ideal.

Measuring real-time changes in mechanical properties is desirable to study dynamic biological processes, which remain inaccessible through conventional methods at cell scales. A major challenge in real-time hydrogel swelling measurements is distinguishing the surrounding water from the water absorbed by the hydrogel sample. Due to having a density and acoustic impedance similar to water after swelling, hydrogel samples (like many biosamples) are especially challenging (contrast issues) to distinguish from water through ultrasound reflectometry. Recently, the GHz ultrasound-based imager has been used to study micro-organisms, such as *C. Elegans*, that require a moist/wet environment to survive, meaning the samples are wet when placed on the ultrasound chip [5]. However, the GHz ultrasound imager is sensitive enough to the difference in the acoustic impedance between the surrounding liquid solution and the micro-organism in the study, creating a contrast difference in the ultrasound image.

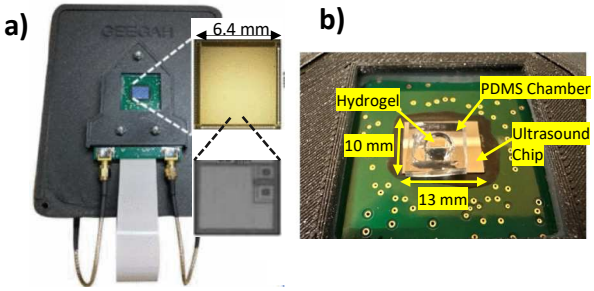

Figure 1: (a) GHz ultrasound reflectometry measurement setup, the imager has a 128x128 array of ~50x50 micron AlN transducers (shown as inset) [6] (b) Closeup ultrasound chip with PDMS chamber, and a l sample.

To overcome the acoustic contrast challenge (similar acoustic properties), we use a differential imaging methodology that offsets the acoustic reflection coefficient of the surrounding water media and the Polydimethylsiloxane (PDMS) barrier used for containing the water from that of the hydrogel, at the start of the experiment.This method allows us to measure the acoustic reflection coefficient change relative to the surrounding media.

DEVICE DESIGN AND OPERATION

Figure 1 shows the GHz ultrasound imager (Geegah LLC) setup consisting of the imager chip, PDMS (Polydimethylsiloxane) sample enclosure, and hydrogel sample. The top surface of the imager chip consists of a Si layer that has a thickness of 750 µm. The imager uses nanosecond pulse trains and resolves nanosecond-level echo data. The transducer timing (transmit and receive) is controlled through a scripting interface (Python), allowing

the imager control and signal processing cointegration, such as image filters, denoising, and contour detection at one interface.

Sample Enclosure Integration

The experiment setup consists of a PDMS open enclosure cured on a polystyrene substrate, peeled off, and then punched and bonded to the imager chip (backside), as shown in Figure 2. The overall dimension of the PDMS enclosure is 10x13 mm^2 (thickness can be adjusted to the diameter of the sample). The punched area is approximately 6.4mm x 6.4mm to match the size of the sensing area of the ultrasound imager chip.

The hydrogel samples are prepared for two experiments. The first experiment is designed to characterize the stiffness of the hydrogel after the swelling is completed (steady state). Using this experiment as proof of concept, the second experiment is designed to characterize the transient change in the acoustic reflection coefficient during the real-time swelling of the hydrogel.

For the first experiment, Super Absorbent Polymer (SAP) based hydrogels (water beads, a commercial product) samples are prepared with deionized water (DI) at concentrations of 50 to 1000 µL/100mg and a dry sample. The samples are kept in a moisture-tight holder (centrifuge tube) with the added water for a day for the swelling to be completed. The prepared samples with different water contents are shown in Figure 3a. The PDMS enclosure is bonded to the Si layer of the ultrasound chip, forming a barrier that holds the sample and any possible leakage from the sample contained.

For the second experiment, a PDMS barrier with an exposed area that is slightly smaller than the sensor area is used. After bonding PDMS to Si, the enclosure is filled with DI water, and then a dry SAP bead is added, allowing the ultrasound measurements from the initial time and during the swelling process.

DATA ACQUISITION AND PREPROCESSING

Ultrasound pulses at ~1.8 GHz with 100 ns duration are generated by the AlN transducers and transmitted through the Si layer to the hydrogel sample. Due to the acoustic impedance difference between the silicon and the sample, a portion of the incident pulse energy is reflected from the sample, creating an echo signal. The transducers pick up the echo from the silicon and sample interface with predictable timing to constitute an echo signal measured in the mV range. The pulse and echo signals are illustrated in Figure 3b. The echo signal amplitude picked up by each transducer provides information for 1 pixel of data. Figure 3c shows an ultrasound image constructed by the received ultrasound echo signals.

This measurement scheme is used to measure five different hydrogel samples from each of the seven different batches with varying water content, and twenty frames of data are acquired for each sample.

The acquired ultrasound image consists of different regions produced by the echo from the silicon-sample interface and the echo from the silicon-air interface. In Figure 3c, the darker region is produced by the echo signal from the silicon-sample interface. In contrast, the lighter yellow region represents the echo signal intensity reflected from the silicon-air interface. For measurement accuracy, the echo signal intensity values should only be obtained from the sample area, which requires signal processing for contour detection. We developed an image processing method by applying filters, thresholding, and the convex hull computation to produce a contour around the sample area. Only the pixels within the contour limits are used to calculate echo signal intensity from the sample.

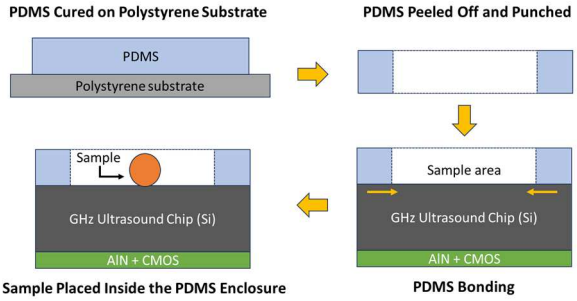

Figure 2: Measurement chamber/enclosure (PDMS) integration for hydrogel/water sample handling on ultrasound imager.

We implemented an automated image processing algorithm to detect the hydrogels as objects in the ultrasound reflection images. To detect the edges of the hydrogel sample, we use fast non-local denoising (`cv2.fastNlMeansDenoising`), Binary thresholding (`cv2.THRESH_BINARY`), Gaussian Blur (`cv2.GaussianBlur`) for reducing the random noise, and adaptive thresholding (`cv2.adaptiveThreshold`) [7]. Finally, by computing the convex hull (`cv2.convexHull`) in the processed frame, the accurate Region of Interest (ROI) is selected. For robustness of the ROI algorithm (Figure 4), only the largest contour is selected, which serves as an additional protection measure for the cases where more than one independent contour can be formed in an image due to contours formed from noise that went unfiltered until the final step.

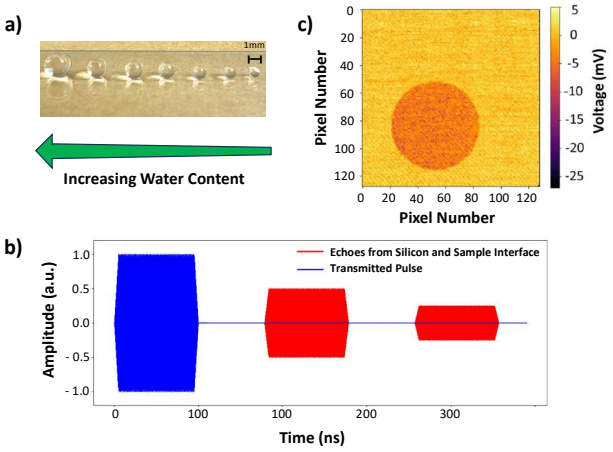

Figure 3: Ultrasound imaging of hydrogel beads. (a) Hydrogel beads with different water content, (b) ultrasound pulse-echo signal, (c) 128x128 pixel unprocessed ultrasound reflected echo image.

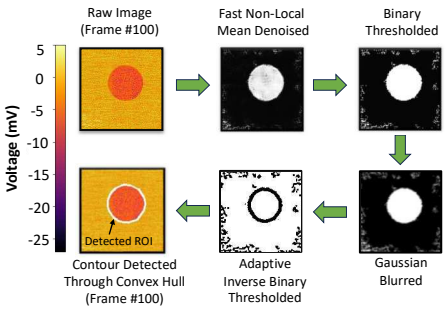

Figure 4: Fully automated object detection and ROI selection algorithm for GHz ultrasound images. All images are 128x128 pixels, covering a 6.4x6.4 mm² field of view.

The magnitude of ultrasound echo is used for determining the acoustic reflection coefficient of the silicon-sample interface. The magnitude of the echo signal from the sample is proportional to the transmitted signal magnitude and the sample/silicon acoustic reflection coefficient. The echo signal magnitude from air can be calculated similarly. Since the transmitted signal magnitude for air and sample is the same, their echo signal magnitudes are equal to the ratio of their acoustic reflection coefficient with silicon. Since the air/silicon reflection coefficient is approximately 1, the ratio of the echo signal magnitudes from air and sample becomes equal to the sample/Si reflection coefficient.

$$\frac{M_{sample,echo}}{M_{air,echo}} = \frac{M_{sample,trans}}{M_{air,trans}} \cdot \frac{\Gamma_{sample/Si}}{\Gamma_{air/Si}} = -\Gamma_{sample/Si} \quad (1)$$

The acoustic reflection coefficient is then used to compute the acoustic impedance of the sample through the analytical formula given in Equation (2). Since the acoustic impedance of Si is 19.6 MRayls, the acoustic impedance of the sample is calculated by using the echo signal measurements obtained from the imager chip.

$$Z_{sample} = Z_{Si} \cdot \frac{(1+\Gamma_{sample/Si})}{(1-\Gamma_{sample/Si})} \quad (2)$$

The acoustic impedance is then used to derive the bulk modulus through the relationship shown in equation (3), which is used for determining the stiffness of hydrogels.

$$K_{sample} = \frac{Z^2_{sample}}{\rho_{sample}} \quad (3)$$

We have used micro-indentation (Mach-1, Biomomentum, Canada) at a velocity of 0.1 mm/s with a flat tip indenter that is 1 mm in diameter (MA655) as a verification method to confirm the ultrasound-based measurements of the elastic properties of the hydrogel samples. Obtaining force-displacement curves and applying the Hertzian Contact theory analytical model, the Young's modulus of samples is computed. The analytical expression obtained from the Hertzian Contact model is shown in Equation (4) [8]. This Young's modulus value is then converted to bulk modulus, assuming a constant mean Poisson's ratio (0.48) [9] for all samples.

$$E_{indentation} = \frac{3}{4} \cdot \frac{FR_{indenter}}{(displacement)^3} \quad (4)$$

$$K_{indentation} = \frac{E_{indentation}}{3(1-2\nu)} \quad (5)$$

RESULTS

Ultrasonic imaging measurements are taken for various hydrogel samples with water contents ranging from zero (dry) to 1000 µL water per 100 mg. Reflection coefficient values are obtained from 20 frames of measurement for each sample by using only the pixel values within the ROI for five different samples (same water content) for each of the seven batches (different water content). Figure 5 shows the distribution of the reflection coefficient data points obtained from 35 experiments. The variation in dry samples is caused by the size of the samples being measured, which only allows a limited number of pixels (fewer than 4 pixels per ROI) to be taken. The plot also displays the ultrasound images of the samples with the detected ROI marked as a green contour overlay. The number of pixels within each ROI is listed on top of the corresponding picture. The ultrasound reflection coefficient data and increasing trend from dry to the highest water content accurately show the hydrogels' increased water content.

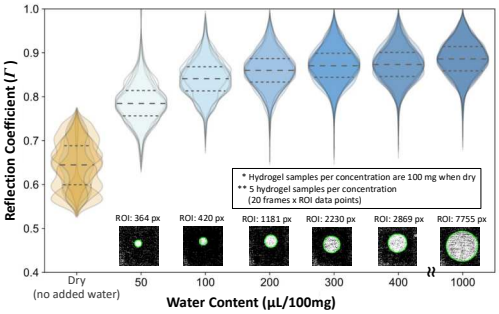

Figure 5: Noninvasive GHz ultrasound metrology for hydrogel water content. The statistical variations (100 measurements per water content) are shown as violin plots, showing overall ~1.5M data points. Each overlaying violin plot shows the measured results of a different sample. The automated ROI (green line) for each water content level is shown as insects—the size of ROI increases by swelling of samples (larger contact area with imager).

The measured ultrasound reflection coefficient image data are used to compute the acoustic impedance using the analytical relationship shown in Equation (2). The acoustic impedance is then used to calculate the bulk modulus using Equation (3). The computed acoustic impedance data and bulk modulus data averaging over five samples for each batch are shown in Figure 6.

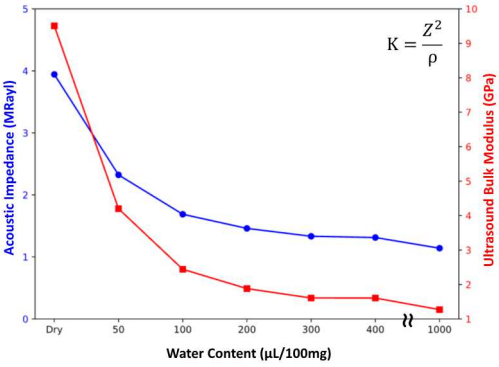

Figure 6: Post-processed ultrasound data for computed acoustic impedance (Z) and bulk modulus (K) averaged (arithmetic mean) over the region of interest of 5 samples from each batch and over 20 frames.

The bulk modulus is measured by the GHz ultrasound setup, and the Young's modulus derived from the force-displacement measurements obtained by the micro-

indentation method. Although the moduli were computed through different models due to the mode of measurements, the overall trend in both data agrees well in a way that indicates a decrease in stiffness with increasing water content. The GHz ultrasonic approach might yield higher moduli owing to the increased stiffening of the gel at GHz frequencies [10]. In contrast, the nanoindentation occurs near zero frequency measurement.

The results of our bulk modulus calculations from both the ultrasound and the micro indentation data show that an increase in water content translates to a decrease in the stiffness of hydrogel samples in an interval within the same order of magnitude for both methods. Figure 7 shows a similar trend in bulk modulus change for both methods.

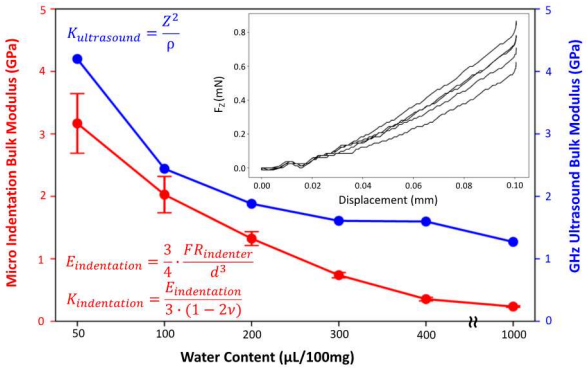

Figure 7: Comparison between the bulk modulus obtained from GHz ultrasound reflectometry and bulk modulus obtained from micro-indentation force-displacement curves. The inset shows a force-displacement of raw data repeated over five samples of hydrogel(1000µL/100mg).

Figure 8 displays the result of applying the reflection coefficient methodology dynamically during the swelling process of the hydrogel. The inset data provides the calibration baseline obtained from the acoustic reflection of the PDMS enclosure and water (no hydrogel sample). The main plot shows the change in the reflection coefficient after the dry sample (SAP bead) is added. The initial drop and the increasing trend are indicators of a sample with a different acoustic impedance being added during measurement. The increasing trend shows an increase in the acoustic reflection coefficient of the sample as it absorbs more water, which agrees with the findings from our measurements with static concentrations.

CONCLUSION

The results from the ultrasound and micro indentation measurements show that with increasing water content, the bulk modulus of hydrogel decreases at a decreasing rate in a range that is within the same order of magnitude for both measurement methods. This correlation verifies GHz ultrasound reflectometry as a potential noninvasive elasticity measurement of the hydrogel. The divergence between the results from the two models for larger samples with more water content requires further investigation of the air gap formation within the hydrogel during swelling. For more accurate processing of the micro indentation data, inverse finite element analysis will be used in future work.

The increasing trend in the acoustic reflection coefficient of the real-time imaging of hydrogel swelling agrees with the results from the samples with static concentrations, as samples with higher static concentrations also yielded a higher reflection coefficient. This indicates that the dynamic measurement successfully displays the change in the acoustic reflection coefficient of the hydrogel as its water content increases.

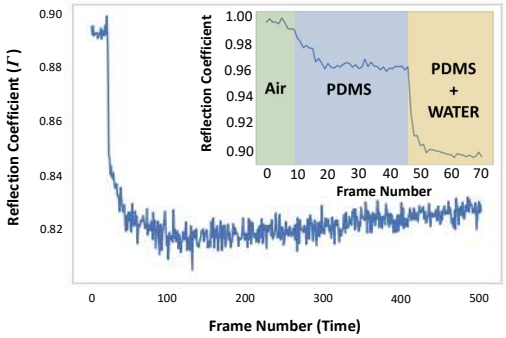

Figure 8: Dynamic hydrogel swelling measurement by GHz ultrasound. Reflection coefficients are normalized to remove the background. The inset shows calibration data.

ACKNOWLEDGEMENTS

This work is partially supported by a Northeastern University TIER 1 award.

REFERENCES

[1] A. M. Kloxin, C. J. Kloxin, C. N. Bowman, and K. S. Anseth, "Mechanical properties of cellularly responsive hydrogels and their experimental determination," *Advanced Materials*, vol. 22, no. 31, pp. 3484–3494, 2010.

[2] Wu, Sheng, et al. "Aluminum nitride piezoelectric micromachined Ultrasound Transducer Arrays for noninvasive monitoring of radial artery stiffness." *Micromachines*, vol. 14, no. 3, 2023, p. 539.

[3] J. Chen *et al.*, "A review of ultrahigh frequency ultrasonic transducers," *Frontiers in Materials*, vol. 8, 2022.

[4] A. Baskota, J. Kuo, S. Ardanuç, and A. Lal, "Compact GHz ultrasonic micro-imager for cells and tissues," *Microscopy and Microanalysis*, vol. 29, no. Supplement_1, pp. 1116–1117, 2023.

[5] J. Kuo *et al.*, "Gigahertz ultrasonic imaging of nematodes in liquids, soil, and Air," *2021 IEEE International Ultrasonics Symposium (IUS)*, 2021.

[6] J. Hwang, A. Baskota, B. Davaji, J. Kuo, and A. Lal, "Gigahertz metamaterial ultrasonic lens characterization using GHZ CMOS integrated ultrasonic micro imager," *2022 IEEE International Ultrasonics Symposium (IUS)*, 2022.

[7] "OpenCV Modules," OpenCV, https://opencv.org/.

[8] A. C. Fischer-Cripps, "Contact mechanics," *Nanoindentation*, pp. 1–20, 2004.

[9] U. Chippada, N. Langrana, and B. Yurke, "Complete mechanical characterization of soft media using nonspherical rods," *Journal of Applied Physics*, vol. 106, no. 6, 2009.

[10] A. Hasanov, M. Prasad, and M. Batzle, "Fluid and rock bulk viscosity and modulus," *SEG Technical Program Expanded Abstracts 2016*, 2016.

CONTACT

*B. Davaji ; b.davaji@northeastern.edu